Recent Advances in Science and Engineering
Web page info: https://rase.yildiz.edu.tr
DOI: 10.14744/rase.2025.0001

Research Article

Effects of DEM overlapping distance on hydrological analysis

Burak BALIKCI[1], Türkay GÖKGÖZ[2*]

[1]*Graduate School of Science and Engineering, Yildiz Technical University, Istanbul, Türkiye*
[2]*Department of Geomatic Engineering, Yildiz Technical University, Istanbul, Türkiye*

ARTICLE INFO

Article history
Received: 4 February 2025
Revised: 19 March 2025
Accepted: 20 March 2025

Key words:
DEM, hydrological analysis, horizontal and vertical positional accuracies, geomorphometric parameters, topographic parameters.

ABSTRACT

Deriving Digital Elevation Models (DEMs) from topographic map data is essentially an interpolation process. So, when a DEM mosaic is obtained from a set of DEMs, elevation errors arise, especially along common boundaries. To solve this problem, DEMs are derived so that they have areas in common with their neighbours, and the elevations of the cells in the common areas, i.e. overlapping areas, are recalculated during mosaicking. A DEM mosaic obtained in this way will be different from the individual DEMs, and the difference will depend on the overlapping distance. In this study, in order to determine the effects of DEM overlapping distance on hydrological analysis, drainage networks and basin boundaries are derived by hydrological analyses on DEM mosaics obtained from 0, 1000, 2000, 3000, 4000, 5000 and 6000 m overlapping DEMs derived from 1:25,000 scale topographic map data, furthermore, horizontal and vertical positional errors of the basins, various geomorphometric and topographic parameters are calculated. Consequently, it can be said that the overlapping distance affects the geometries of the derived drainage networks and basin boundaries and, accordingly, the horizontal positional accuracies, and geomorphometric and topographic parameters of the basins, but do not affect the vertical positional accuracies.

Cite this article as: Balıkcı B, Gökgöz T. Effects of DEM overlapping distance on hydrological analysis. Recent Adv Sci Eng 2025;5:1.

INTRODUCTION

The process of collecting land surface elevation data is essentially a sampling process because it is not possible to record all points on the Earth's surface. There are two sampling approaches as systematic and adaptive. In the systematic approach, elevation points are measured at regular intervals. The final product is a matrix containing elevation values and is often called a Digital Elevation Model (DEM) and is used widely in many studies such as hydrological analysis in Geographic Information Systems (GIS).

There are three main data sources for DEMs: measurement of point coordinates (latitude, longitude, and elevation or *x, y, z* values) by geodetic methods, contours from printed topographic maps if vector datasets are not available, digitization of features such as streams, lakes, etc., and interpretation of image data obtained from aircraft or satellite platforms [1].

When deriving DEMs from topographic maps, in cases where the volume of data used is much higher than the data processing capacity of the GIS tool, DEMs are derived on a map basis and then merged to obtain the DEM mo-

***Corresponding author.**
*E-mail address: gokgoz@yildiz.edu.tr

saic of the study area. However, when DEMs are derived on a map basis and these DEMs are merged, the problem of edge effects, in other words, elevation errors along the DEM boundaries, occurs. The process of deriving DEMs from topographic maps is essentially an interpolation process since the elevation values of DEM cells are calculated by interpolation from the topography and hydrography data given as input. The effect of the interpolation process increases towards the boundaries. For this reason, it is best to merge the overlapping DEMs, i.e. DEMs with common areas along their boundaries. Common areas can be formed by expanding the original map boundaries by a certain amount [2].

Ozulu and Gökgöz investigated the problem of edge effects that occur in DEMs derived from 1:25,000 scale topographic data on a map basis and suggested that as a solution, DEMs should be derived from topographic data in the map boundaries expanded by 6000 m in each direction and these DEMs should be clipped based on the map boundaries expanded by 3000 m in each direction [3]. Six more analyses were conducted by Ozulu to identify whether the 6000 m and 3000 m overlapping distances were appropriate. The boundaries of two 1:25,000 scale topographic maps were expanded by 1000 m each time to create 12 novel map boundaries; the map boundaries, including the common boundary of the two maps, were converted into a line feature, and then each line feature was expanded by 100 m to have 13 test areas. DEMs were derived at the original boundaries, 3000 m expanded boundaries, and 6000 m expanded boundaries, and the DEMs derived at the 3000 m expanded map boundaries were merged. A point feature was created at the centre of each DEM cell in the test areas, the value of each DEM cell was assigned to the point feature created at the centre of that cell, and thus a series of test points known with their locations and elevations were obtained in each test area. The elevation differences calculated at the test points in each test area were examined and the average elevation error in each test area was calculated. As a result, it was found that producing DEMs by expanding the original map boundaries by 6000 m and merging these DEMs after clipping them based on the original map boundaries expanded by 3000 m a) increased the number of points with elevation difference less than 10 cm, b) decreased the number of points with elevation difference greater than 3 m, c) decreased the number of points with elevation difference greater than 5 m and d) reduced the mean elevation error, thus confirming the suitability of the 6000 m and 3000 m distances [4].

In previous studies conducted in the literature, DEMs were generally derived from remote sensing data, and the width of the common areas (overlapping distance) was determined depending on various factors (purpose of the study, data sources, DEM resolution, shape and size of the study area, etc.) such as a) number of cells [5], b) distance [6-9] and c) percentage [10-16].

This study aimed to determine the effects of DEM overlapping distance on hydrological analysis. To this end, hydrological analyses were carried out on DEM mosaics obtained with 0, 1000, 2000, 3000, 4000, 5000 and 6000 m overlapping DEMs derived from 1:25,000 scale topographic map data; drainage networks and basin boundaries were derived; horizontal and vertical positional errors of the basins, and various geomorphometric and topographic parameters were calculated.

STUDY AREA AND DATA

The study area is the first level sub-basin number 2 of the Western Mediterranean Basin, which is one of the 25 basins located in Turkey (Fig. 1 and 2). The Western Mediterranean Basin is approximately 20,332 km^2 in the mid-latitude zone (between latitudes 36.13° and 37.67°) with an east-west extension (between longitudes 27.23° and 30.59°). The study area is 1,131 km^2.

The elevation (contour and elevation point) and hydrography (intermittent stream, perennial stream, channel, lake, coastline) data from TOPO25 databases that were produced by the General Directorate of Mapping (GDM) were used in this study (Fig. 3). These were vector data in 3D point and line geometry types. The main contour interval was 10 m, and the vertical positional (elevation) accuracy

Figure 1. Western Mediterranean Basin.

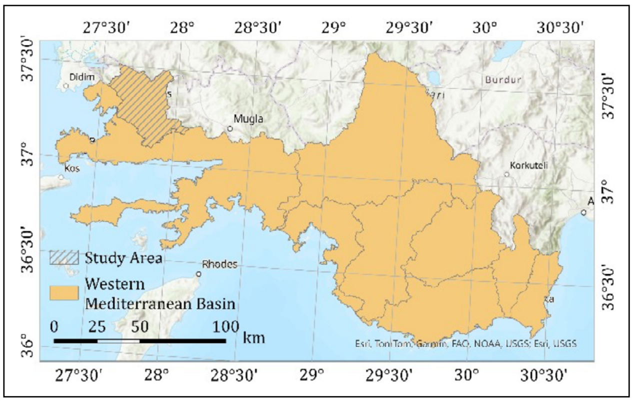

Figure 2. Study area: sub-basin no. 2 [17]

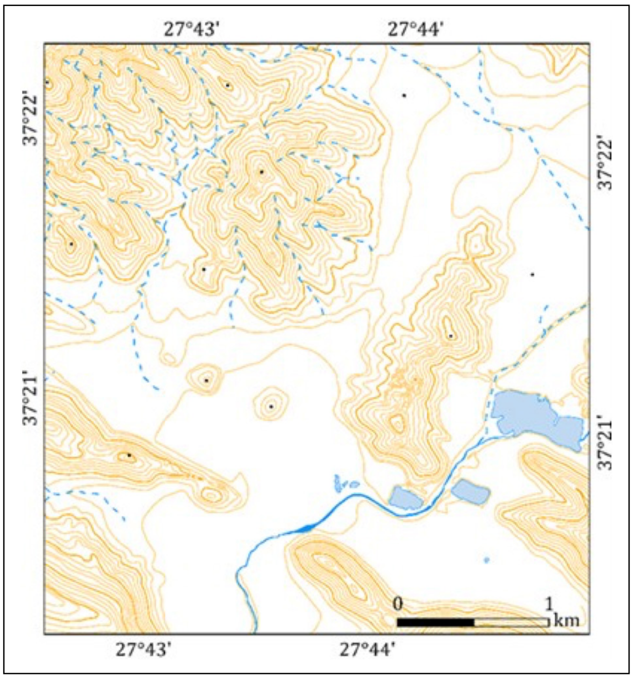

Figure 3. Contour, elevation point, intermittent stream, perennial stream, and lake data from TOPO25 database belonging to a small area.

was ±3 m at 95% confidence level. The horizontal (planimetric) and vertical (elevation) positional accuracies of the hydrography data were ±4 m and ±3 m, respectively, at 95% confidence level [17-19].

These data originally positioned in the geographic coordinate system were repositioned in the Albers equal-area conic projection by Gökgöz et al. with the idea that length and area information are more important than angle (shape) information for hydrological analyses (Table 1). Also, by using the existing GIS tools and special AutoLISP scripts, various geometric and topological errors were removed, i.e. the data was cleaned, and a merged database with six feature classes was formed [17].

Table 1. Projection and reference coordinate system parameters

Projection	Albers
Linear Unit	Meter
False Easting	0.0
False Northing	0.0
Central Meridian	35.0
Standard Parallel 1	36.5
Standard Parallel 2	41.0
Latitude of Origin	0.0
Geographic Coordinate System	WGS 1984
Datum	D WGS 1984

DERIVATION OF DIGITAL ELEVATION MODELS

Firstly, from the map-based data in the TOPO25 database, non-overlapping DEMs were derived at the original map boundaries by using the ArcGIS/TopoToRaster tool. In this tool, the interpolation method developed by Hutchinson [20] based on the "discretized thin plate spline technique" is employed. In this method, although the primary input data is the contours, additional elevation and hydrography data are also used to adjust the elevations of DEM points corresponding to drainage lines while removing spurious pits. For this reason, the DEM obtained with this method is called "hydrologically corrected DEM". Thus, it is possible to derive drainage networks in continuous form. The 17 non-overlapping DEMs obtained in this way were merged by using the ArcGIS/Mosaic tool to obtain a DEM mosaic (DEM0) (Figs. 4 and 5).

DEM mosaics of overlapping DEMs were obtained through the following four steps.

Step 1: The original map boundaries were expanded by 1000, 2000, 3000, 4000, 5000 and 6000 m (Fig. 6).

Step 2: The data in the merged database were clipped based on the 6000 m expanded boundaries, and 6000 m overlapping DEMs were derived from these data. The values of the "Output Extent" parameter of the ArcGIS/TopoToRaster tool were determined to be multiples of 10 meters and did not go outside the DEM boundaries because when these values are determined automatically based on the DEM boundaries, they are not multiples of 10 meters, which causes the formation of residual cells along the DEM boundaries and inconsistencies in terms of alignment between neighbouring DEM cells (Fig. 7).

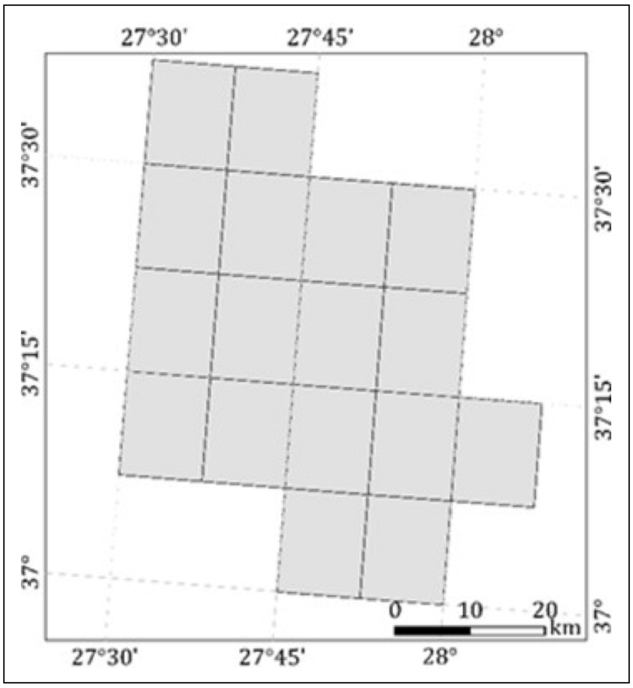

Figure 4. Original map boundaries.

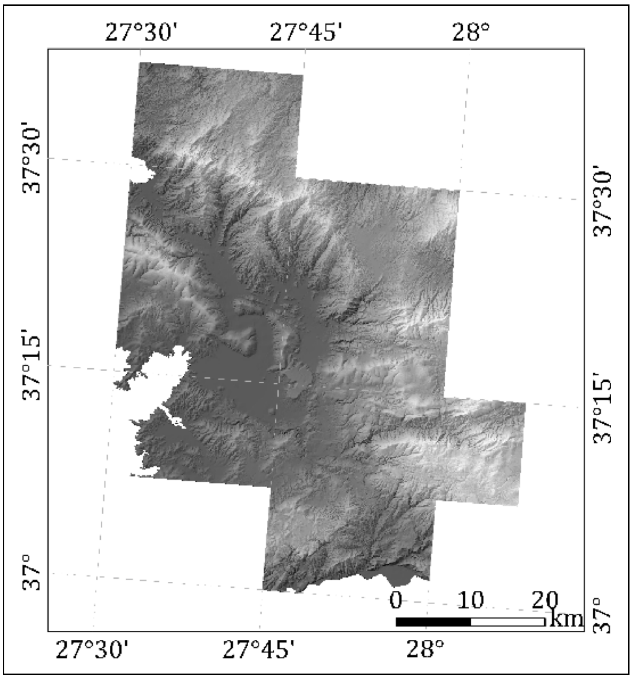

Figure 5. DEM mosaic of non-overlapping DEMs (DEM0).

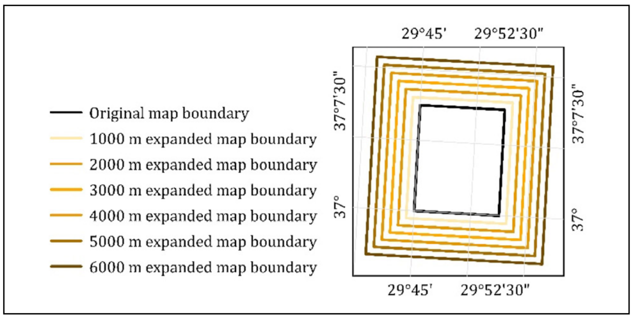

Figure 6. Original and expanded map boundaries.

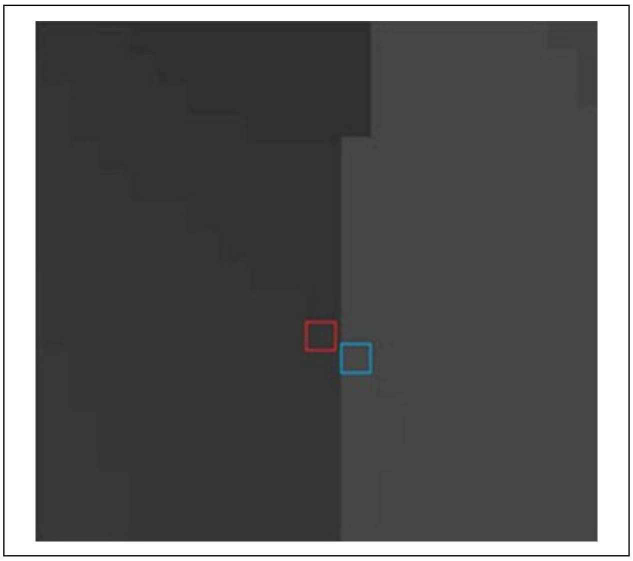

Figure 7. The alignment mismatch problem between neighbouring DEM cells [17].

Step 3: 6000 m overlapping DEMs were clipped based on 1000, 2000, 3000, 4000 and 5000 m expanded boundaries, and 1000, 2000, 3000, 4000 and 5000 m overlapping DEMs were obtained.

Step 4: 1000, 2000, 3000, 4000, 5000 and 6000 m overlapping DEMs were merged to obtain 1000, 2000, 3000, 4000, 5000, and 6000 m DEM mosaics (DEM1000, DEM2000, DEM3000, DEM4000, DEM5000 and DEM6000) respectively (Figs. 8-13). When merging the overlapping DEMs by using the ArcGIS/Mosaic tool, "Mean" was selected for the "Mosaic Operator" parameter, in other words, the elevation value of each cell in the overlapping area was calculated as the arithmetic average of the elevation values of two cells at the same location in the overlapping DEMs.

HYDROLOGICAL ANALYSES: DERIVATION OF DRAINAGE LINES AND BASIN BOUNDARIES

Basin boundaries are mainly derived from a DEM over the following steps [21, 22]:

- Filling the sinks,
- Determining the flow directions,
- Calculating the flow accumulation values, and
- Deriving the drainage networks and determining the basin boundaries based on the flow accumulation values.

The process of deriving drainage lines and basin boundaries was performed with the ArcGIS/ArcHydro tool in accordance with the flow chart in Figure 14. As the stream threshold, 1% of the maximum flow accumulation value, which is also offered to the user by the "Stream Definition"

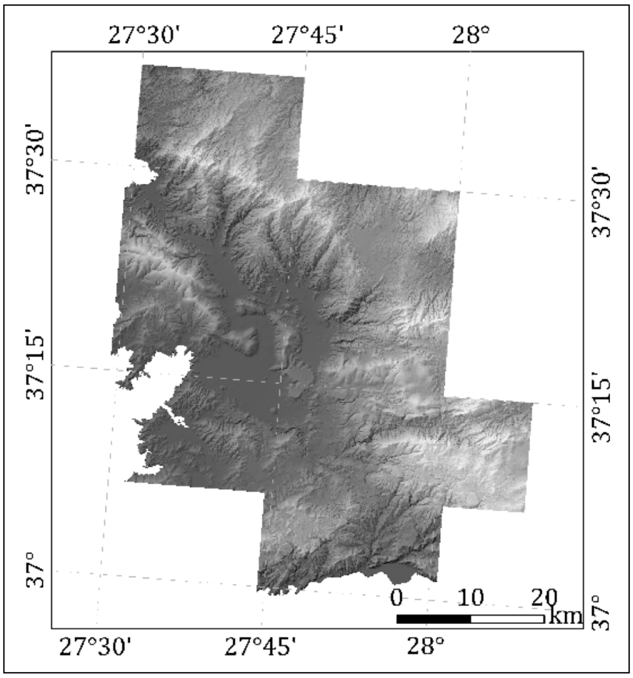

Figure 8. DEM mosaic of 1000 m overlapping DEMs (DEM1000).

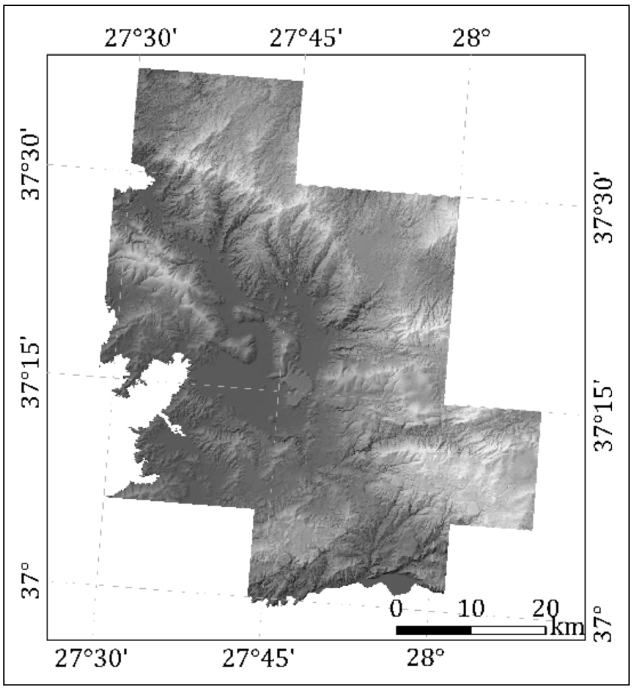

Figure 9. DEM mosaic of 2000 m overlapping DEMs (DEM2000).

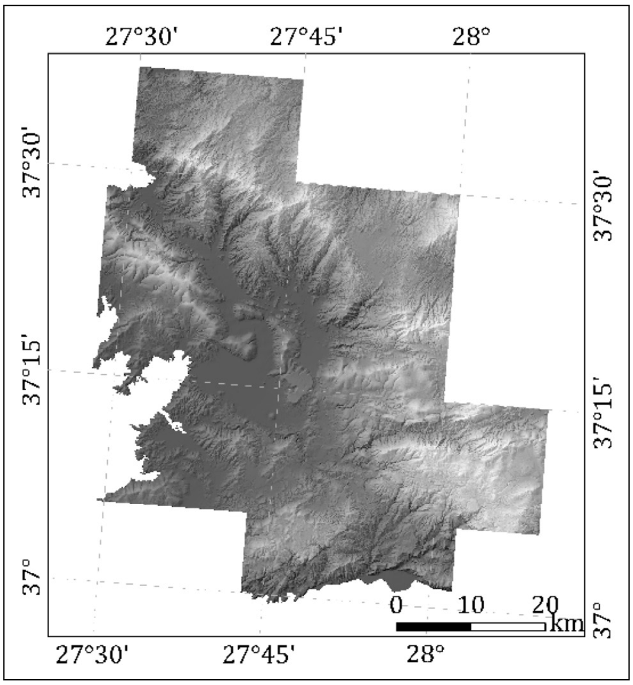

Figure 10. DEM mosaic of 3000 m overlapping DEMs (DEM3000).

tool, was used [23]. All the derived drainage networks are shown in Figure 15 in a superimposed manner. To indicate the geometric differences, the drainage networks in the region depicted by a red rectangle in Figure 15 are shown in Figure 16 at larger scale. The geometric characteristics of the drainage networks are given in Table 2 as well.

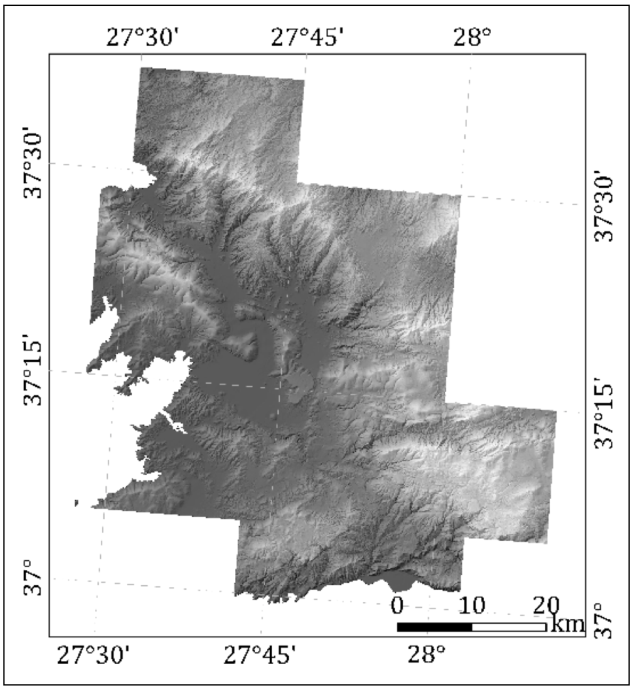

Figure 11. DEM mosaic of 4000 m overlapping DEMs (DEM4000).

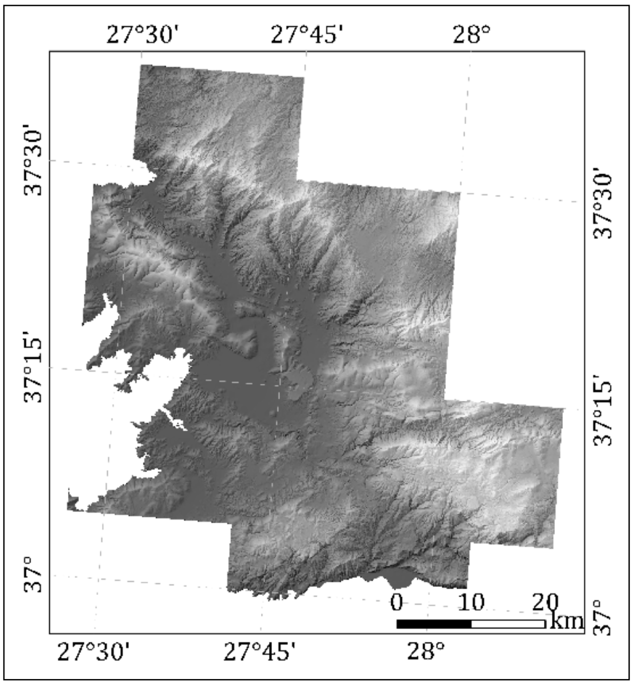

Figure 12. DEM mosaic of 5000 m overlapping DEMs (DEM5000).

As a result, it is seen that the DEM cell elevations change depending on the overlapping distances and for this reason, the geometric characteristics of the derived drainage networks are different. However, no direct or inversely proportional relationship can be established between the overlapping distance and the number of drainage lines and the

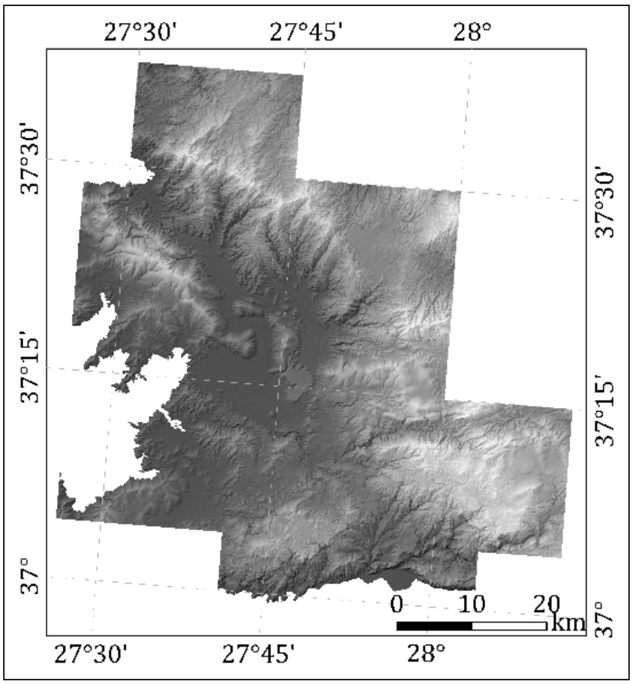

Figure 13. DEM mosaic of 6000 m overlapping DEMs (DEM6000).

total drainage length: while the overlapping distance increases linearly, the number of drainage lines and the total drainage length neither increase nor decrease linearly. The smallest number of drainage lines is derived from DEM0, DEM3000 and DEM4000; the average number of drainage lines is derived from DEM1000, DEM2000 and DEM5000; the highest number of drainage lines is derived from DEM6000. The shortest drainage network is derived from DEM1000; the drainage network with the closest length to the average is derived from DEM5000; the longest drainage network is derived from DEM6000.

The flow chart of deriving the basin boundaries is given in Figure 17. All the derived basin boundaries are shown in Figure 18 in a superimposed manner. To indicate the geometric differences, the basin boundaries in the region depicted by a red rectangle in Figure 18 are shown in Figure 19 at larger scale. The geometric characteristics of the basins are given in Table 3 as well.

As a result, since the derived drainage networks are different, the basin boundaries are also different, and this is an expected situation. However, it cannot be argued that there is neither a direct nor an inversely proportional relationship between the overlapping distance and the basin boundary length and area: while the overlapping distance increases linearly, the basin boundary length and area neither increase nor decrease linearly. The shortest basin boundary is derived from DEM6000, the longest basin boundary is derived from DEM0 and DEM4000, and the basin boundary with the closest length to the average is derived from DEM3000. Based on the basin areas, the smallest basin is derived from DEM3000, the largest

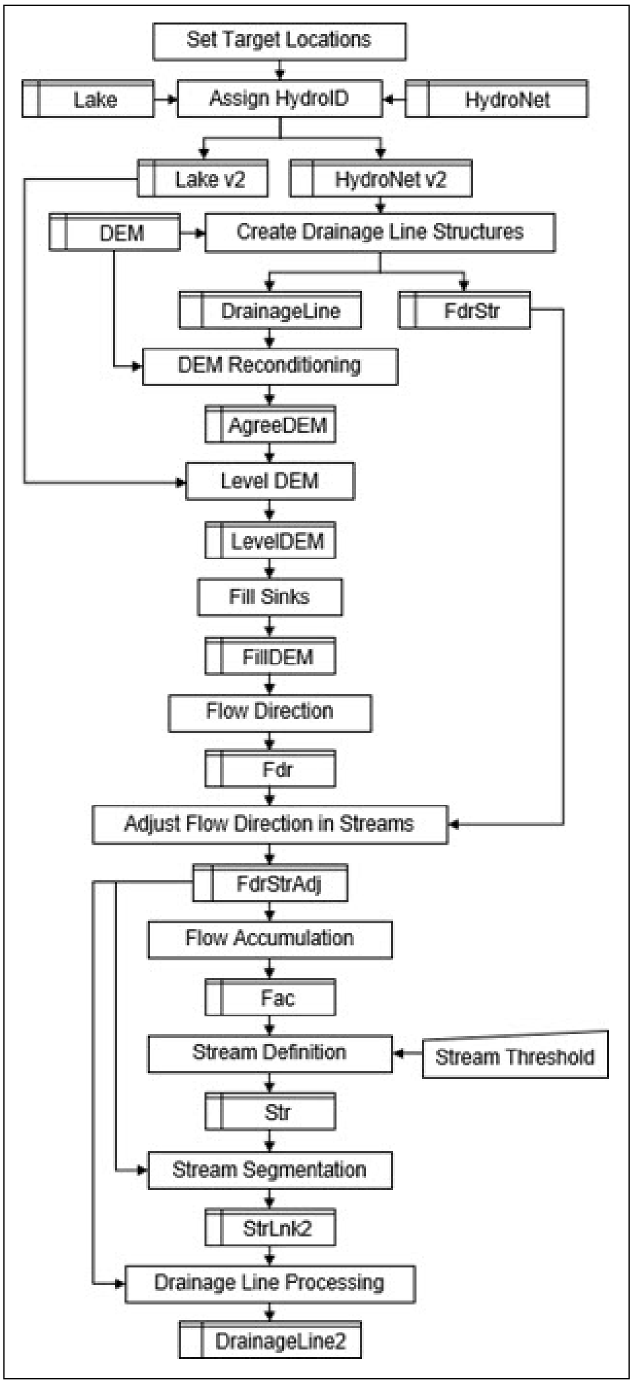

Figure 14. Derivation of drainage lines.

basin is derived from DEM1000, and the basin with the closest area to the average is derived from DEM5000.

There is no relationship between the basin boundary length and the basin area. As the basin boundary length increases, the basin area may decrease and vice versa. This situation is natural and depends on the number and length of convex and concave shapes occurring along the basin boundary. If the number and length of concave shapes increase, the area decreases (Fig. 20).

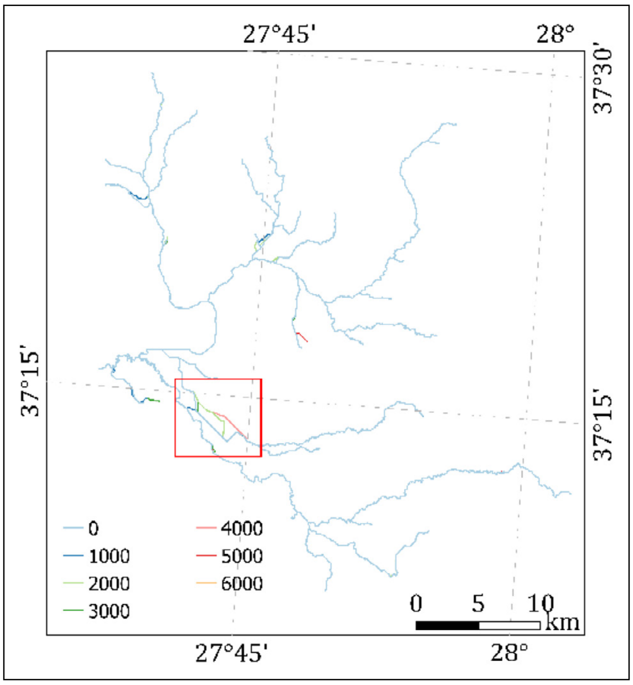

Figure 15. Drainage networks derived from DEM mosaics.

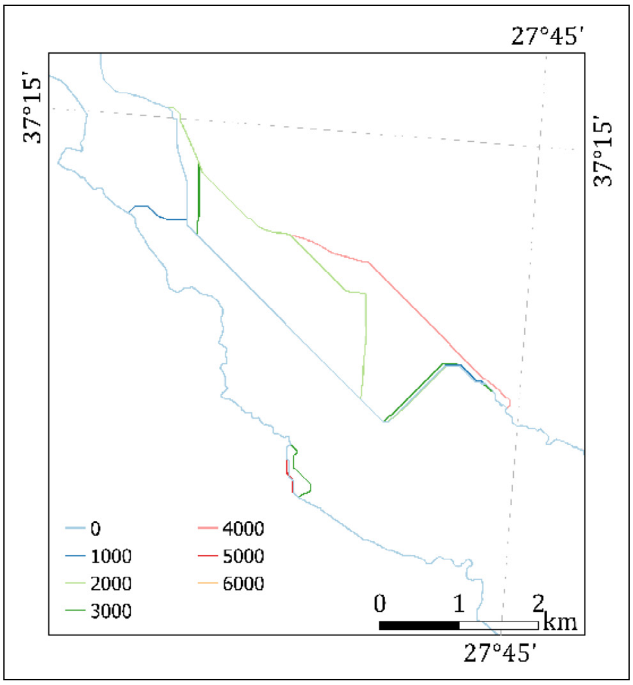

Figure 16. Geometric differences between drainage networks.

Table 2. Geometric characteristics of the drainage networks

DEM	Overlapping distance [m]	Elevation [m]			Flow accumulation value [km²]	Number of drainage lines	Total drainage length [km]
		Min.	Avg.	Max.			
DEM0	0	0.00	439.82	1418.09	11,3128	55	331.61
DEM1000	1000	0.00	439.68	1418.09	11,3128	57	330.37
DEM2000	2000	0.00	440.47	1418.09	11,3128	57	332.93
DEM3000	3000	0.00	440.34	1418.09	11,3128	55	333.73
DEM4000	4000	0.00	439.12	1418.09	11,3128	55	332.33
DEM5000	5000	0.00	437.09	1418.09	11,3128	57	333.41
DEM6000	6000	0.00	435.04	1418.09	11,3128	59	339.03

For example, the boundary length of the basin derived from DEM1000 is smaller than the boundary length of the basin derived from DEM0, but the area of the basin derived from DEM1000 is larger than the area of the basin derived from DEM0, which means that there are more concave shapes along the boundary of the basin derived from DEM0. For this reason, only a relative assessment can be made by comparing the boundary lengths and areas of the basins. To make an absolute assessment, a basin boundary that can be considered as "ground truth" is needed. In this study, the basin drawn in three dimensions on stereo models by an experienced operator working in GDM was accepted as the "ground truth" and was mentioned as basinGDM (Fig. 21). In this context, it is understood that basin6000 is closer to the basinGDM in terms of border length and basin3000 in terms of area (Table 3).

EFFECTS OF DEM OVERLAPPING DISTANCE

The horizontal root mean square errors (RMSE) of the basin boundaries were calculated to determine the effects of DEM overlapping distance on the horizontal positional accuracies of the basins, and the vertical (elevation) RMSEs of the DEMs from which the basin boundaries were derived were calculated to determine the effects of DEM overlapping distance on the vertical positional accuracies of the basins. Also, various geomorphometric and topographic parameters were calculated to determine the geomorphometric and topographic effects of DEM overlapping distances.

Horizontal Positional Accuracies of the Basins

To determine the effects of DEM overlapping distance on the horizontal positional accuracies of the basins, the horizontal RMSEs of the basin0, basin1000, basin2000, ba-

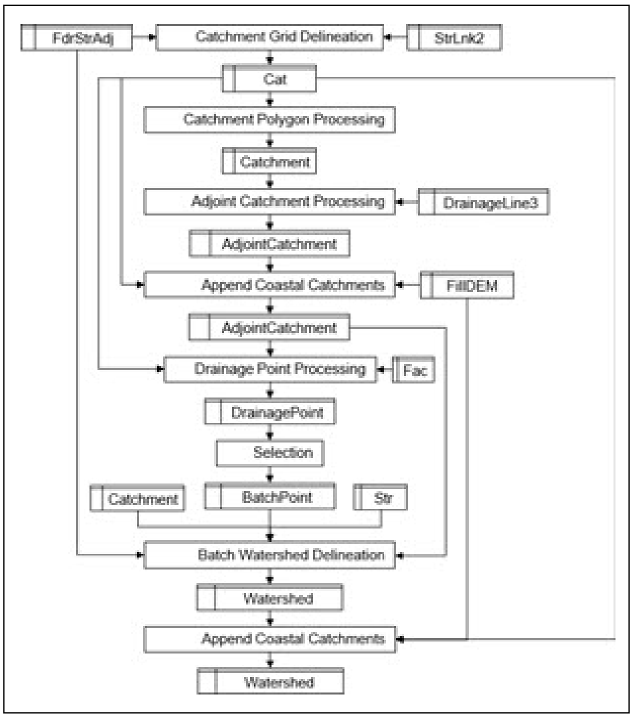

Figure 17. Derivation of basin boundaries.

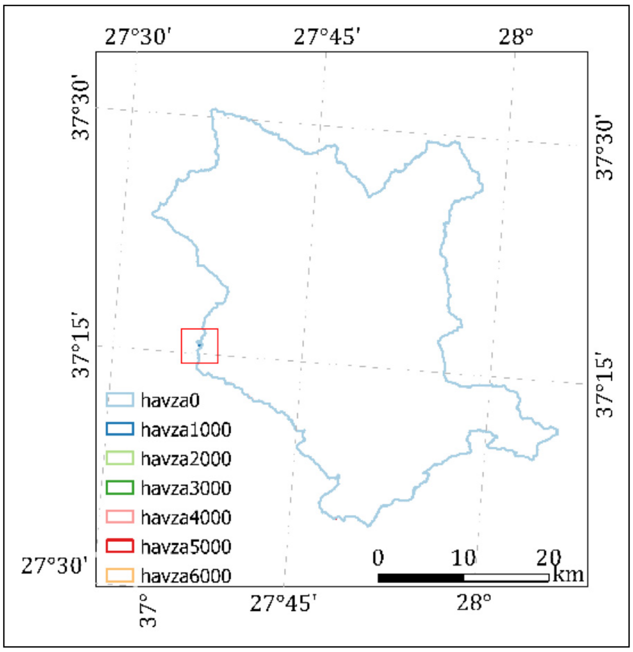

Figure 18. Basin boundaries derived from DEM mosaics.

sin3000, basin4000, basin5000 and basin6000 concerning the ground truth basin (basinGDM) were calculated by using the following equation.

$$m_l = \sqrt{\frac{\sum_{i=1}^{n} d_i^2}{n}} \qquad (1)$$

In this equation, d_i is the horizontal positional difference between each point (measurement point) of the ground truth basin boundary and the derived basin (basin0, basin1000, basin2000, basin3000, basin4000, basin5000 and basin6000) boundary; n is the number of measurement (horizontal distance) or measurement points. The horizontal positional differences (d_i) were measured in the AutoCAD environment by using a script, which was written with AutoLISP, the macro programming language of AutoCAD, and print on an Excel page. The horizontal RMSEs (m_l) were calculated in Excel with these measurements. The horizontal RMSEs are given in Table 4. As a result, basin0, basin3000 and basin6000 gave the smallest values (233.56 m) in terms of horizontal positional difference, and basin0 and basin3000 gave the smallest values (16.26 m) in terms of horizontal positional error. In this context, it can be argued that basin0 and basin3000 are the closest basins to the ground truth (basinGDM) in terms of horizontal positional error.

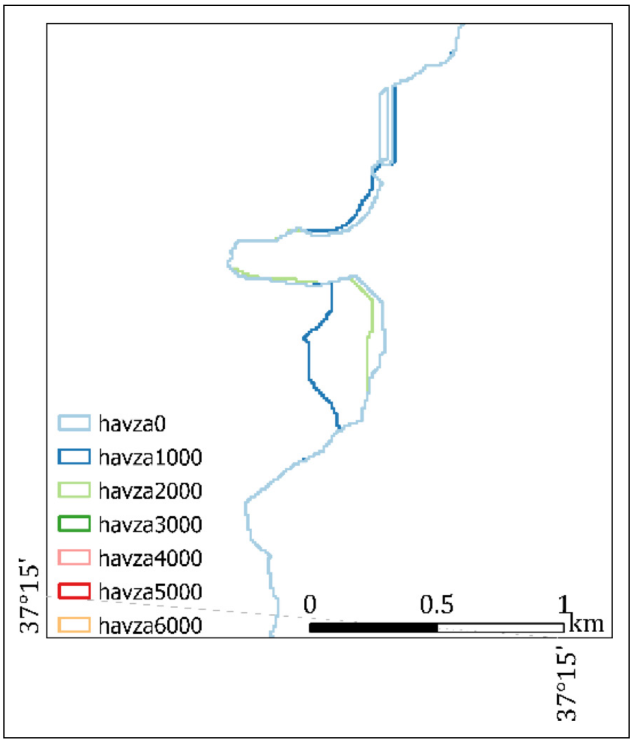

Figure 19. Geometric differences in basin boundaries.

Table 3. Geometric characteristics of basin boundaries

Basin	DEM overlapping distance [m]	Basin boundary length [km]	Basin area [km²]
basinGDM	-	239.14	1131.01
basin0	0	294.02	1131.26
basin1000	1000	293.14	1131.36
basin2000	2000	293.24	1131.26
basin3000	3000	293.18	1131.25
basin4000	4000	294.02	1131.26
basin5000	5000	293.10	1131.27
basin6000	6000	292.94	1131.29

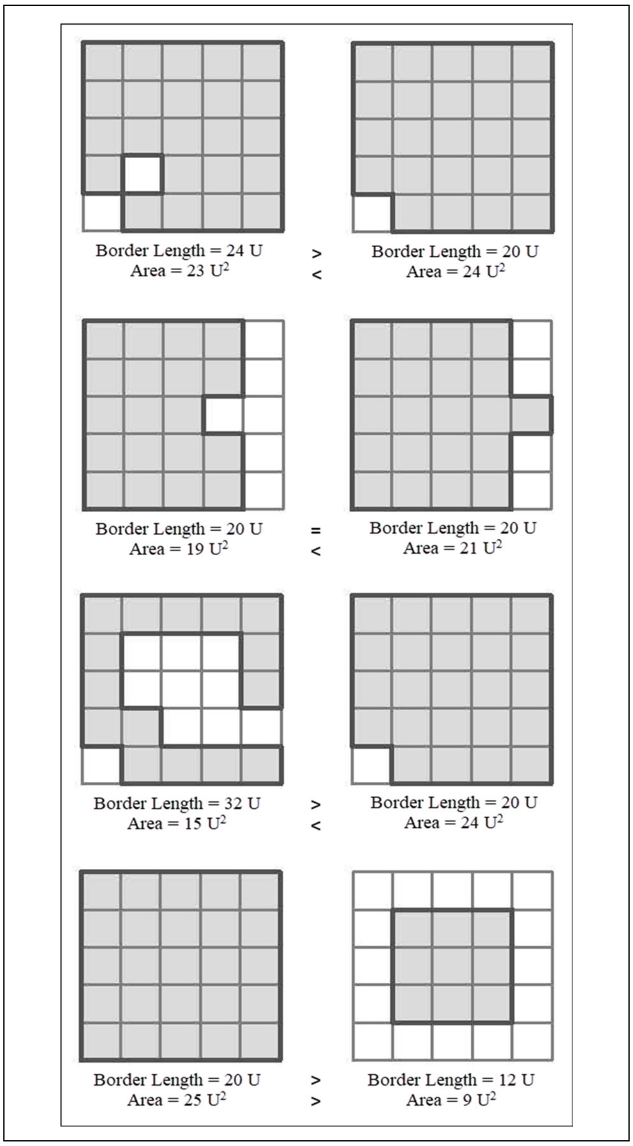

Figure 20. Boundary length-area relationship.

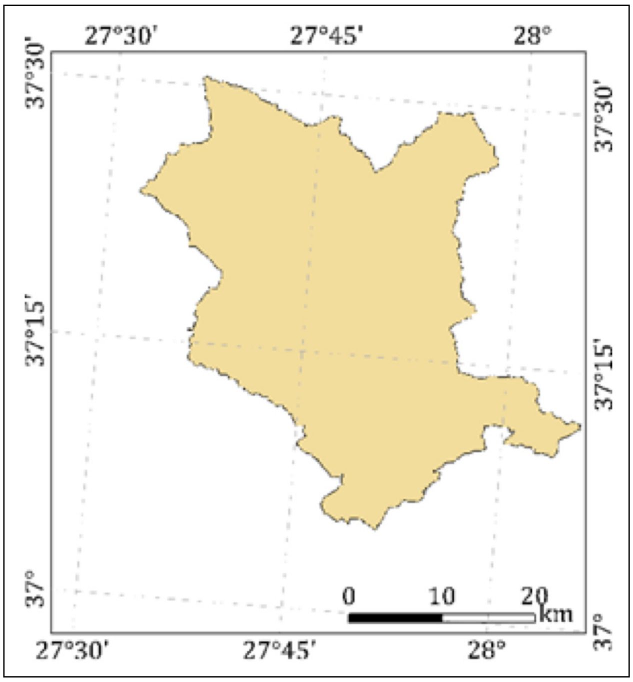

Figure 21. Ground truth for the basin boundary (basinGDM).

Vertical Positional Accuracies of the Basins

When calculating the horizontal RMSEs of the basins, point features are created at the junctions (vertices) of consecutive line segments of basinGDM boundary (the ground truth) and if more than one point is created at a junction, all but one are deleted. Since the basinGDM boundary is three-dimensional, these points are also three-dimensional. In the calculation of the vertical (elevation) RMSE of a derived basin using the following equation, the elevations of these points are accepted as "ground truth values", and the values of the cells corresponding to these points in the DEM from which the basin was derived (on which these points are located) are accepted as "measurements".

Table 4. Horizontal RMSEs of the basins

Basin	Number of basin boundary points	Horizontal positional difference (d_i) [m]		Horizontal RMSE (m_l) [m]
		Min.	Max.	
basin0	10838	0.00	233.56	16.26
basin1000	10838	0.00	248.11	17.88
basin2000	10838	0.00	248.11	17.88
basin3000	10838	0.00	233.56	16.26
basin4000	10838	0.00	248.11	17.88
basin5000	10838	0.00	248.11	17.88
basin6000	10838	0.00	233.56	16.52

$$m_h = \sqrt{\frac{\sum_{i=1}^{n} dh_i^2}{n}} \quad (2)$$

In this equation, dh_i is the difference between the measurement and the ground truth value, and n is the number of measurements or point features.

The vertical RMSEs are given in Table 5. As a result, the calculated minimum and maximum vertical positional differences at the basinGDM boundary points are the same, but the vertical RMSEs of basin0, basin1000, basin2000, basin3000, basin5000, and basin6000 are the same (2.83 m), while the vertical RMSE of basin4000 is 0.01 m smaller. In this context, it can be argued that basin4000 is closer to basinGDM in terms of vertical positional error.

Geomorphometric Parameters

The quantitative definition and analysis of the geometric characteristics of the Earth's surface is defined as geomorphometry. Geomorphometry uses a series of numerical measurements that usually extract surface parameters and characteristics from DEMs. For example, based on the ruggedness and slope parameters, the Earth can be divided into three as flat, hilly, and mountainous. Ruggedness is a number that varies between "0" and "1". If the ruggedness number is "0", it indicates flat areas, and if it is "1", it indicates mountainous areas [24]. The parameters and their definitions are given in Table 6, and the values calculated for each derived basin are given in Table 7. As a result, it is understood that the drainage density, ruggedness and slope characteristics of all basins are the same; in other words, the differences in drainage networks and basin boundaries do not affect the geomorphometric parameters.

Topographic Parameters

Topographic parameters such as shape factor, bifurcation ratio, drainage frequency, length of the main flow path, harmonic slope, time of concentration and hypsometric curve are needed in various basin-based analyses [25].

The topographic parameters of the basins derived from DEM mosaics were automatically calculated in this study by using programs written in Python programming language by Gökgöz et al. [26] and recorded in the attribute tables. Topographic parameters are briefly explained as follows in accordance with the algorithmic design approach [17, 27].

The basin shape factor is computed as the square of the length of the main flow path divided by the basin area. The bifurcation ratio is computed based on the ordering that is done according to Horton's method. The stream order is a measure of the degree of stream branching within a basin. Each length of stream is indicated by its order (for example, first-order, second-order, etc.). A first-order stream is an unbranched tributary, and a second-order stream is a tributary formed by two or more first-order streams. A third-order stream is formed by two or more second-order streams, and in general, an *n*th-order stream is a tributary formed by two or more streams of order (n-1) and streams of lower order. The bifurcation ratio is defined as the ratio of the number of streams of any order to the number of streams of the next higher order. The mean bifurcation ratio is obtained by arithmetically averaging all bifurcation ratio. The drainage frequency is defined as the total number of stream segments per unit area. The drainage frequency is computed in the form of ratio of total stream segments with same Horton's order obtained to basin area. The distance

Table 6. Geomorphometric parameters [24]

Name/Description	Symbol/Formula
Basin area	A_b [km^2]
Basin crest	$Cr_b=Z_{max}$ [m]
Length of basin boundary	P_b [km]
Total length of drainage network	L_d [km]
Drainage density	$D_b=L_d/A_b$ [km/km^2]
Contour interval	e [m]
Total length of contours	L_c [km]
Basin relief	$R_b=Z_{max}-Z_{min}$ [m]
Ruggedness number	$R_n=D_b\ R_b$
Melton's ruggedness number	$M=R_b/\sqrt{(A_b)}$
Drainage slope	$S_b=e\ L_c\ /\ A_b$

Table 5. Vertical RMSEs of the basins

Basin	Number of basin boundary points	Vertical positional difference (dh_i) [m]		Vertical RMSE (m_h) [m]
		Min.	Max.	
basin0	10838	0.00	31.82	2.83
basin1000	10838	0.00	31.82	2.83
basin2000	10838	0.00	31.82	2.83
basin3000	10838	0.00	31.82	2.83
basin4000	10838	0.00	31.82	2.82
basin5000	10838	0.00	31.82	2.83
basin6000	10838	0.00	31.82	2.83

measured along the main flow path from the basin outlet to the end of the main flow path is the length of the main flow path. The basin slope is computed as the difference in elevation between the end points of the main flow path divided into ten equal parts. The harmonic slope is computed by using the slope values obtained in this way. Time of concentration is the longest time required for a particle to travel from the basin divide to the basin outlet. The hypsometric curve is a description of the cumulative relationship between elevation and the area within elevation intervals. In this study, the digital elevation model is classified according to the determined elevation interval. In the digital elevation model classified, number of cells in every class are determined. Number of cells in every class is multiplied with a cell area and thus area of every class is computed. These area values are counted up cumulatively. The elevation data are also classified in the same way. The hypsometric curve is created with the area and elevation values obtained. While assessing the curve formed, approximately 10% parts are deducted from start and end of the curve.

The formulas of the topographic parameters are given in Table 8. The results obtained for each basin are shown in Table 9 and Figures 22-28. As a result, it is understood that differences in drainage networks and basin boundaries affect all topographic parameters - except for the harmonic slope.

CONCLUSION

To determine the effects of DEM overlapping distance on hydrological analysis, drainage networks and basin boundaries were derived in this study by performing hydrological analyses on DEM mosaics of 0, 1000, 2000, 3000, 4000, 5000, and 6000 m overlapping DEMs derived from 1:25,000 scale topographic map data, and various geomorphometric and topographic parameters were calculated along with horizontal and vertical positional accuracies of the basins.

The results could be evaluated as follows.

- The derived drainage networks were different.

Table 7. Geomorphometric parameters of the basins

Parameters	Basin						
	0	1000	2000	3000	4000	5000	6000
A_b	1131.26	1131.36	1131.26	1131.26	1131.26	1131.27	1131.29
Cr_b	1403.10	1403.10	1403.10	1403.10	1403.10	1403.10	1403.10
P_b	294.02	293.14	293.24	293.18	294.02	293.10	292.94
L_d	331.61	330.37	332.93	333.73	332.33	333.41	339.03
D_b	0.2931	0.2920	0.2943	0.2950	0.2938	0.2947	0.2997
e	10	10	10	10	10	10	10
L_c	31010.63	31014.44	31017.24	31016.86	31016.87	31018.56	31020.93
R_b	1403.10	1403.10	1403.10	1403.10	1403.10	1403.10	1403.10
R_n	0.41	0.40	0.41	0.41	0.41	0.41	0.42
M	1.32	1.32	1.32	1.32	1.32	1.32	1.32
S_b	0.03	0.03	0.03	0.03	0.03	0.03	0.03

Table 8. Topographic parameters [27]

Name/Description	Symbol/Formula
Length of the main flow path	U_{em} [m]
Shape factor	$B_k = U_{em}^2 / A$ (A: Basin area)
Bifurcation ratio	$Ç = S_i / S_{(i+1)}$ (S_i: Number of streams of Horton's order-i)
Drainage frequency	$D_f = (\sum_{i=1}^{m} S_i)/A$ (m: Number of streams)
Harmonic slope	$e_h = \left(10/\sum_{i=1}^{10}\left(1/\sqrt{(\Delta e)_i}\right)\right)^2$ [$(\Delta e)_i$: The slope of the part-i of the main flow path divided into 10 equal parts]
	$(\Delta e)_i = (\Delta y)_i/\Delta u$ $\Delta u = U_{em}/10$ [$(\Delta y)_i$: Elevation difference along the part-i; Δu: Length of each part]
Time of concentration	$T_t = 0{,}0195(U_{em}/\sqrt{(e_{em})})^{0{,}77}$
	$e_{em} = U_{em}/R_b$ (e_{em}: Slope of the main flow path; R_b: Basin relief [m])

Table 9. Topographic parameters of the basins

Parameters	Basin						
	0	1000	2000	3000	4000	5000	6000
U_{em}	82,936.20	82,936.20	82,936.20	83,127.33	83,133.19	82,956.20	83,402.83
B_k	6.08	6.08	6.08	6.11	6.11	6.08	6.15
Ç	11.00	4.04	4.03	4.07	4.07	3.97	3.99
D_f	0.46	0.18	0.18	0.18	0.18	0.18	0.18
e_h	0.02	0.02	0.02	0.02	0.02	0.02	0.02
T_t	559.19	559.19	559.19	560.82	560.84	559.35	553.88

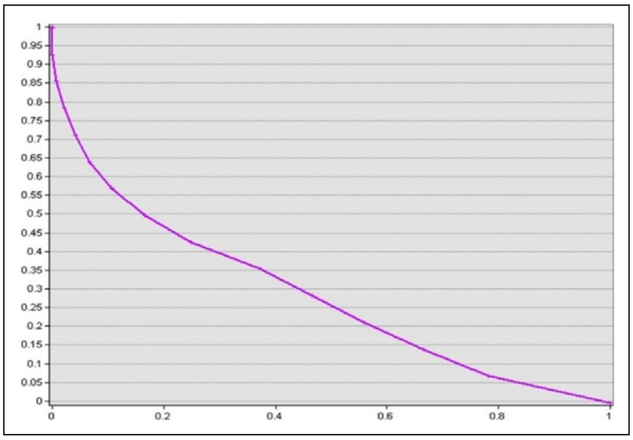

Figure 22. Hypsometric curve of basin0.

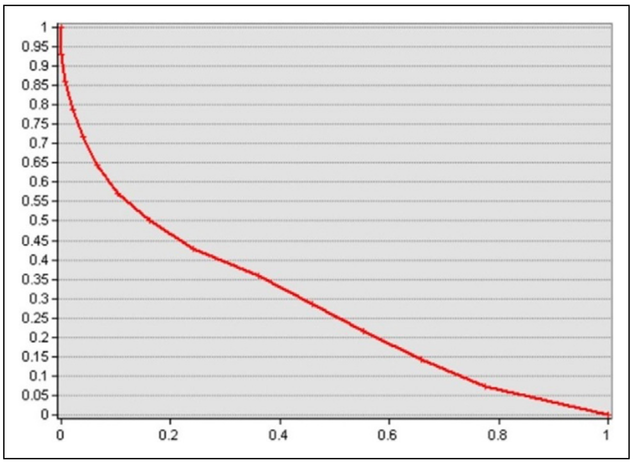

Figure 23. Hypsometric curve of basin1000.

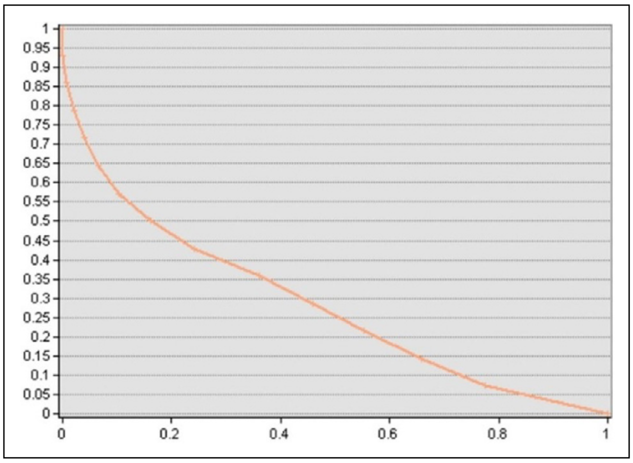

Figure 24. Hypsometric curve of basin2000.

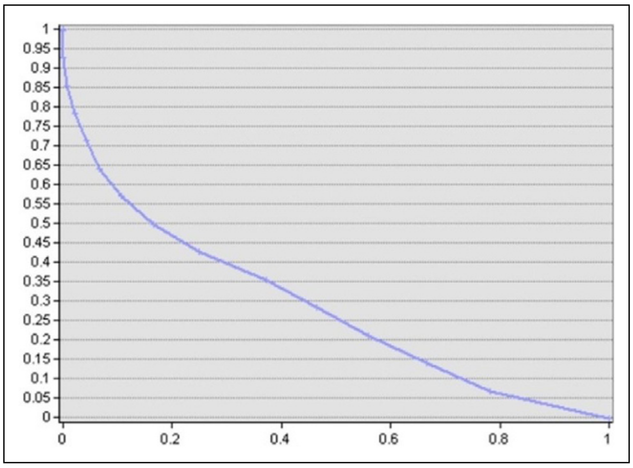

Figure 25. Hypsometric curve of basin3000.

- There was no relationship between the overlapping distance, the number of drainage lines and the total drainage length.
- There was no relationship between the overlapping distance and the basin boundary length and area.
- The horizontal positional accuracies of the basins derived from DEM mosaics of non-overlapping and 3000 m overlapping DEMs were higher than the others.
- Although the vertical positional error of the six basins was the same, the vertical positional error of the basin derived from the DEM mosaic of 4000 m overlapping DEMs was 0.01 m smaller. For this reason, it could be assumed that the vertical positional accuracies of all basins are almost the same.
- The drainage density, ruggedness and slope characteristics of all basins were the same, but the topographic parameter values were different, except for the harmonic slope.

In conclusion, it can be argued that DEM overlapping

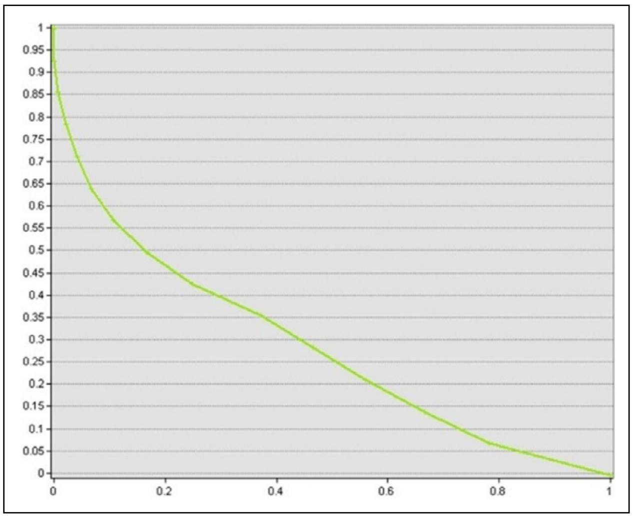

Figure 26. Hypsometric curve of basin4000.

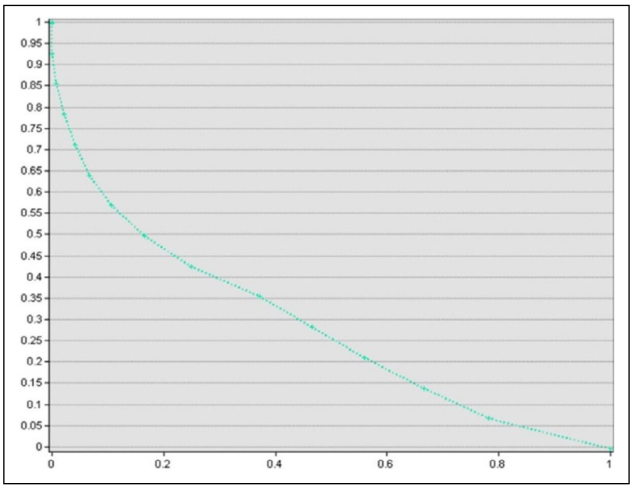

Figure 27. Hypsometric curve of basin5000.

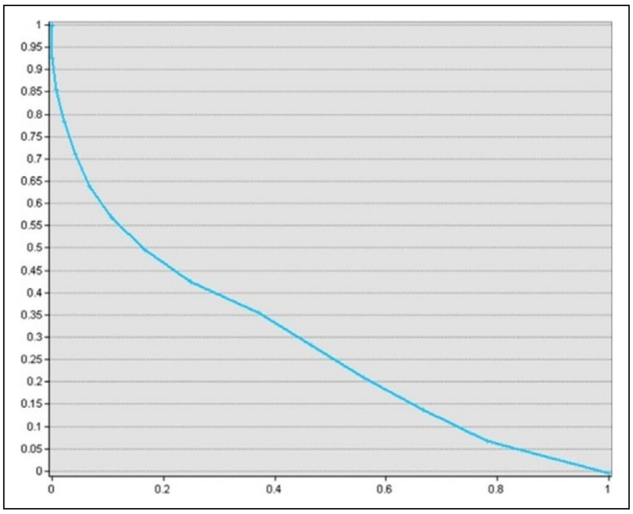

Figure 28. Hypsometric curve of basin6000.

distances have an impact on the geometries of the derived drainage networks and basin boundaries and, in this context, the horizontal positional accuracies of the basins and the geomorphometric and topographic parameters but does not affect the vertical positional accuracies.

ACKNOWLEDGMENTS

The present study was supported by the Scientific and Technological Research Council of Türkiye (TUBITAK) under project number 115Y411 and by the General Directorate of Mapping under project number 1912310112.

AUTHORSHIP CONTRIBUTIONS

Concept: Türkay Gökgöz, Design: Türkay Gökgöz, Supervision: Türkay Gökgöz, Data: Burak Balıkcı and Türkay Gökgöz, Analysis: Burak Balıkcı and Türkay Gökgöz, Literature search: Burak Balıkcı and Türkay Gökgöz, Writing: Türkay Gökgöz and Burak Balıkcı, Critical revision: Türkay Gökgöz.

DATA AVAILABILITY STATEMENT

The published publication includes all graphics and data collected or developed during the study or the projects mentioned above.

CONFLICT OF INTEREST

The author declared no potential conflicts of interest with respect to the research, authorship, and/or publication of this article.

ETHICS

There are no ethical issues with the publication of this manuscript.

REFERENCES

[1] Nelson AD, Reuter HI, Gessler P. DEM production methods and sources. In: Hengl T, Reuter HI, editors. Geomorphometry: concept, software, applications. Developments in Soil Science. Vol. 33. p. 65–85. [CrossRef]

[2] Gökgöz T, Erdoğan M, Seyrek K, Ozulu İM. Determining the high accuracy boundaries of Western Mediterranean Basin. Turk J Civ Eng 2019;30:9073–9105. [Turkish] [CrossRef]

[3] Ozulu İM, Gökgöz T. Edge effects between the borders of two adjacent digital elevation models. Int Symp Appl Geoinf (ISAG-2019); 2019 Nov 7–9; İstanbul, Türkiye

[4] Ozulu İM. Obtaining and coding of drainage basin

objects with high geometric accuracy [dissertation]. İstanbul: Yildiz Technical University; 2023. [Turkish]

[5] Mills S, McLeod P. Global seamline networks for orthomosaic generation via local search. ISPRS J Photogramm Remote Sens 2013;75:101–111. [CrossRef]

[6] Barnard PL, Hoover D. A seamless, high-resolution coastal digital elevation model (DEM) for southern California. US Geol Surv Data Ser 2010;487:8. [CrossRef]

[7] Foxgrover AC, Barnard PL. A seamless, high-resolution digital elevation model (DEM) of the north-central California coast. US Geol Surv Data Ser 2012;684:11. [CrossRef]

[8] Howat IM, Negrete A, Smith BE. The Greenland Ice Mapping Project (GIMP) land classification and surface elevation data sets. Cryosphere 2014;8:1509–1518. [CrossRef]

[9] Rizzoli P, Martone M, Gonzalez C, Wecklich C, Tridon DB, Bräutigam B, et al. Generation and performance assessment of the global TanDEM-X digital elevation model. ISPRS J Photogramm Remote Sens 2017;132:119–139. [CrossRef]

[10] Hasegawa H, Matsuo K, Koarai M, Watanabe N, Masaharu H, Fukushima Y. DEM accuracy and the base to height (B/H) ratio of stereo images. Int Arch Photogramm Remote Sens 2000;33:356–359.

[11] Costantini M, Malvarosa F, Minati E, Zappitelli E. A data fusion algorithm for DEM mosaicking: building a global DEM with SRTM-X and ERS data. IEEE Int Symp Geosci Remote Sens 2006 Jul 31–Aug 4; Denver, CO, USA. [CrossRef]

[12] Buckley SJ, Schwarz E, Terlaky V, Howell JA, Arnott RWC. Terrestrial laser scanning combined with photogrammetry for digital outcrop modelling. Int Arch Photogramm Remote Sens Spatial Inf Sci 2009;38:75–80.

[13] James MR, Robson S. Mitigating systematic error in topographic models derived from UAV and ground-based image networks. Earth Surf Proc Land 2014;39:1413–1420. [CrossRef]

[14] Bertin S, Friedrich H, Delmas P. A merging solution for close-range DEMs to optimize surface coverage and measurement resolution. Photogramm Eng Rem S 2016;82:31–40. [CrossRef]

[15] Bohlin J, Bohlin I, Jonzén J, Nilsson M. Mapping forest attributes using data from stereophotogrammetry of aerial images and field data from the national forest inventory. Silva Fennica 2017;51:1–18. [CrossRef]

[16] Groom J, Bertin S, Friedrich H. Evaluation of DEM size and grid spacing for fluvial patch-scale roughness parameterisation. Geomorphology 2018;320:98–110. [CrossRef]

[17] Gökgöz T, Erdoğan M, Seyrek K, Ozulu İM. Developing an original methodology intended for determination of the river basin/sub-basin boundaries and codes with perspective of European Union Directives. Final Rep TUBITAK Proj No 115Y411. 2017. [Turkish]

[18] Erdoğan M, Toz G. Digital Elevation Model (DEM) accuracy and production costs. 5th Symp Natl Soc Photogramm Remote Sens Türkiye (TUFUAB 2009); 2009 Feb 4–6; Ankara, Türkiye. [Turkish]

[19] Öztürk E, Koçak E. Accuracy investigation of digital elevation models derived at different scales and methods from various sources. Harita Dergisi 2007;137:25–41. [Turkish]

[20] Hutchinson MF. A new procedure for gridding elevation and stream data with automatic removal of spurious pits. J Hydrol 1989;106:211–232. [CrossRef]

[21] Li ZL, Zhu Q, Gold C. Digital terrain modeling: principles and methodology. Boca Raton (FL): CRC Press; 2005. p. 323

[22] Chang KT. Introduction to geographic information systems. 5th ed. New York (NY): McGraw-Hill; 2006. p. 447.

[23] Oliveira F, Furnans J, Maidment DR, Djokic D, Ye Z. Arc Hydro: GIS for water resources. In: Maidment DR, editor. Arc Hydro: GIS for Water Resources. Redlands (CA): ESRI Inc.; 2002. Vol. 1. p. 55–86.

[24] Şen A. The applicability of artificial intelligence methods for the selection/elimination process to the stream networks in cartographic generalization [dissertation]. İstanbul: Yildiz Technical University; 2013. Turkish.

[25] Yaman MB, Kaya S, Güvenç H, Yayla Y. Developing tools for computation of basin topographic parameters in GIS [Master Thesis]. İstanbul: Yildiz Technical University, Dept. of Geomatic Engineering; 2016. Turkish.

[26] Gökgöz T, Yayla Y, Yaman MB, Güvenç H, Kaya S. Developing tools for computation of basin topographic parameters in GIS. 3rd Int GeoAdvances Workshop / ISPRS Workshop Multi-dimension Multi-scale Spatial Data Model; 2016 Oct 16–17; İstanbul, Türkiye.

[27] Şen Z. Water science basic topics. İstanbul: Su Vakfı Press; 2002. 227 p. Turkish.